Micro-Raman spectroscopy of rock paintings from the Galb Budarga and Tuama Budarga rock shelters, Western Sahara.

Mercedes Iriarte[a*], Antonio Hernanz[a], José María Gavira-Vallejo[a], Andoni Sáenz de Buruaga[b], Santiago Martín[c]

[a]Universidad Nacional de Educación a Distancia (UNED), Departamento de Ciencias y Técnicas Fisicoquímicas, Facultad de Ciencias, Paseo de la Senda del Rey 9, E-28040 Madrid, Spain.
[b]Universidad del País Vasco (UPV/EHU), Departamento de Geografía, Prehistoria y Arqueología, Facultad de Letras, Tomás y Valiente s/n, 01006 Vitoria-Gasteiz, Spain.
[c]Universidad Nacional de Educación a Distancia (UNED), Departamento de Física Matemática y de Fluidos, Facultad de Ciencias,
Paseo Senda del Rey 9, E-28040 Madrid, Spain

*Corresponding author: Mercedes Iriarte, Departamento de Ciencias y Técnicas Fisicoquímicas, Facultad de Ciencias, UNED. Paseo de la Senda del Rey 9, E-28040 Madrid, Spain. E-mail: meririarte@madrid.uned.es.
Tel. +34 91 3987391, fax +34 91 3986697

A. Hernanz: ahernanz@ccia.uned.es

J.M. Gavira-Vallejo: jm.gavira@ccia.uned.es

Andoni Saénz de Buruaga: andoni.buruaga@ehu.eus

Santiago Martín: smartin@dfmf.uned.es

Abstract

Rock paintings of two recent discovered rock shelters, Galb Budarga and Tuama Budarga, from the southeastern area of the Western Sahara, Sahrawi Arab Democratic Republic, have been studied by micro-Raman spectroscopy and scanning electron microscopy coupled with energy dispersive X-ray spectrometry in order to characterize the composition of the materials present in the painting panels. An unusual white pigment has been used in the zoomorphic pictographs of the Galb Budarga shelter which main components are the anhydrite ($CaSO_4$) polymorphs I and II. Red and orange zoomorphic figures and ancient Berber scripts have been painted in the Tuama Budarga rock shelter. Haematite (α-Fe_2O_3) is the main component of the paints used; amorphous carbon and different manganese oxides have also been detected. Accretions of gypsum ($CaSO_4.2H_2O$) and anhydrite have been observed on the shelter wall used to paint. α-Quartz (α-SiO_2), albite ($NaAlSi_3O_8$), dolomite, $CaMg(CO_3)_2$, calcite ($CaCO_3$) and traces of hydroxylapatite ($Ca_{10}(PO_4)_6(OH)_2$) have been identified in the rocks supporting the paintings of both sites. Layers of calcium oxalates, whewellite ($CaC_2O_4.H_2O$) and weddellite ($CaC_2O_4.(2+x)H_2O$, $x \leq 0.5$) cover the pictorial panels of these rock shelters. A microestratrigraphic study of the paint used in the Tuama Budarga shelter revealed that the pigment layer is bracketed between oxalate layers.

Keywords: Rock art painting, micro-Raman spectroscopy, anhydrite, haematite.

1. Introduction

In the last two decades Raman spectroscopy has become a powerful tool for the study of prehistoric rock art paintings [1]. As a non destructive technique that offers molecular information, even to discriminate mineral polymorphs, Raman spectroscopy has reached a relevant analytical position in this field. Our research group, collaborating with archaeologists and prehistorians has analyzed rock paintings from different parts of the world since years [1-3]. Micro-Raman spectroscopy is particularly efficient to identify the microscopic and heterogeneous composition of pictorial materials, substrata, accretions, contaminants, their granular size and microstratigraphic distribution. Deterioration processes, conservation and authenticity of the rock art are also aims of these studies. After our previous studies in Europe, Asia and America, two rock shelters, Galb Budarga and Tuama Budarga, with pictographs depicted in their walls, and located in the Tiris area of Western Sahara, Sahrawi Arab Democratic Republic (Fig. S1), are an excellent opportunity to study African rock art paintings. They have been hidden under dessert sand (Figs.S2 and S3) for an unknown time, and consequently they are an attractive subject to study. In addition, the Berber script observed in their walls is a valuable written legacy of North African people that merits consideration. Microscopic techniques like micro-Raman spectroscopy (μ-Raman), scanning electron microscopy coupled with energy dispersive X-ray spectrometry (SEM/EDX), polarised light microscopy (PLM) and microstratigraphic studies of thin cross sections of paint samples are very useful to characterize the composition and distribution of the materials present in rock art painting panels [1-6]. Therefore, they

have been applied in this work to identify the pictorial materials used in these pictographs, as well as those of the rocks supporting the paintings and the surfaces of the painted areas.

2. Archaeological background

Galb Budarga and Tuama Budarga rock art sites were discovered on 2011 by one of the authors of the present work (Andoni Sáenz de Buruaga) during an archaeological campaign of the University of the Basque Country and the Culture Department of the Government of the Sahrawi Arab Democratic Republic [7-9]. These sites were found in the south-eastern end of Western Sahara, inside the Sahrawi Arab Democratic Republic and close to the Mauritanian border. These rock shelters, separated 3750 m, are part of the NE-SW Galabt Duguech mountain alignment, located a few kilometres west of Duguech, in the South East sector of the Tiris Sahrawi region (Fig. S1). Both cavities have different types of pictographs, and were made using different colours. Nevertheless, all of them can be included into the Libyco-Berber artistic period of the Western Sahara ornamental production. The Galb Budarga shelter is decorated with white animal figures, Fig.1a, an unusual rock art colour. However, the Tuama Budarga shelter contains zoomorphic figures and ancient Berber scripts in different red and orange colour-scheme shades, Fig. 1b-1e. Despite these differences, both repertories are chrono-stylistically related with the classically denominated Libyco-Berber stage of the Sahrawi artistic sequence, i.e. a period of time in which the "tifinagh" inscriptions would have their culminating development in this part of the Western Sahara, between about the first millennium BC to midway through the first millennium AD [10,11]. Nevertheless, some chromatic overlays observed on the central panel of the Galb Budarga rock shelter, like those observed in other sites of the same southern area of the Sahrawi Tiris, could reveal older depictions in red Tuama Budarga script than in Galb Budarga white pictures [12].

3. Material and methods

3.1. Sample collection

Specimens of paints with different colours, as well as of the rocky substrata from both sites have been extracted, according to a protocol previously described [13], for laboratory analyses. Appropriated characteristics of the rock surface, paint representativeness and archaeological relevance have been considered to select the sampling points. Specimens of the rock (GB1) and the white paint (GB2) have been extracted from the Galb Budarga painting panel. Specimens of Tuama Budarga rock shelter have also been removed and it could be distinguished five different colour shades: pale orange (TB1), dark orange (TB5), pale red (TB4), red (TB3) and dark red (TB2).

3.2. Instrumental

All the samples were investigated with no previous mechanical or chemical treatment. Descriptions of the instruments used for the μ-RS, SEM/EDX and PLM studies, as well as the preparation of the thin polished cross-sections of paint specimens, have been described elsewhere [6,14]. Specific experimental details of this work are reported next. The μ-Raman spectroscopic study has been carried out with a Jobin Yvon HORIBA LabRam-IR HR-800 laboratory spectrograph coupled to an Olympus BX41 microscope. The 632.8 nm line of a He/Ne laser was used for Raman excitation with an effective power of 1.51 mW (50× LWD objective lens) measured at the sample position. The average spectral resolution in the Raman shift range of 100-1700 cm^{-1} was 1 cm^{-1} (focal length 800 mm, grating 1800 grooves/mm, and confocal pinhole 100 μm). The lateral resolving power at the specimen in these conditions is 2~4 μm (50× LWD objective lens). Depending on the spectral background of fluorescence radiation and the intensity of the Raman signals an integration time of between 2 and 10 s and from 16 to 36 spectral accumulations were used in order to achieve an acceptable signal-to-noise ratio. The sine bar linearity of the spectrograph was adjusted using the fluorescent lamps of the lab (zero order position) and the lines at 640.22 and 837.76 nm of a Ne lamp. The confocality of the instrument was refined using the 519.97 cm^{-1} line of a silicon wafer. Wavenumber shift calibration was accomplished with 4-acetamidophenol, naphthalene and sulphur standards [15] over the range 150-3100 cm^{-1}. This result in a wavenumber mean deviation of $\Delta\nu_{cal}$-$\Delta\nu_{obs}$ = -1.21 ± 0.71 cm^{-1} ($t_{Student}$ 95%). The software package GRAMS/AI v.7.00 (Thermo Electron Corporation, Salem, NH, USA) was used to assist with the wavenumber peak-picking and baseline procedures.
The micromorphology and distribution of the components in the TB3 specimens have been observed with a Hitachi S-3000N scanning electron microscope equipped with an Everhart-Thornley detector of secondary electrons with an operating resolution of 3 nm. X-ray microanalyses (EDX) of the specimens were carried out with an energy dispersive X-ray spectrometer (Rontec Xflash Detector 3001) coupled to the scanning electron microscope, Peltier-refrigerated and with the Be window removed.
Polished thin cross sections (thickness 30 μm) of some specimens have been prepared by means of a matrix of Microtek epoxi resin. A petrographic microscope Leica DM2500 with polarised light has been used to obtain microphotographs of these cross sections. They have been used for microstratigraphic studies.

4. Results and discussion

Besides the strong spectral background of fluorescence radiation observed in some spectra, significant Raman bands could be distinguished and assigned to different components. The results obtained are summarised in Table 1.

4.1. Galb Budarga

Raman spectra of the rock supporting the paintings of this site indicates the presence of α-quartz (α-SiO_2), dolomite ($CaMg(CO_3)_2$), albite ($NaAlSi_3O_8$), haematite (α-Fe_2O_3) [16-18], calcium sulphates like gypsum ($CaSO_4.2H_2O$), Fig. 2, and anhydrite ($CaSO_4$).

Hydroxylapatite ($Ca_5(PO_4)_3OH$) micro-crystals have also been detected in the substratum. Bands of this calcium phosphate are observed at 445, 606, 963, 1032, 1058 and 1070 cm^{-1}, Fig. 3A. The strong band at 963 cm^{-1} is assigned to the symmetric stretching mode of the $(PO_4)^{3-}$ anion, whereas the band at 1070 cm^{-1} is assigned to carbonate group (CO_3^{2-}) inclusions [19,20]. The expected O-H stretching band of hydroxylapatite at 3572 cm^{-1} [19] is overlapped with the very broad O-H stretching Raman bands of water molecules from whewellite ($CaC_2O_4.H_2O$) between 3200 and 3700 cm^{-1}, Fig. 3Ac. Hydroxylapatite is the main component of human and animal bones [19,20]. About a 70% of bone weight is due to hydroxylapatite, a 22% to proteins like collagen and an 8% to water molecules. It is known that the biological hydroxylapatite is a non estecheometric molecule with inclusions of carbonate (CO_3^{2-}) and hydrogenphospate $(HPO_4)^{2-}$ anions and other ions like Na^+, Mg^{2+}, Sr^{2+}, K^+, Cl^- y F^-. In the Fig. 4 the Raman spectra shows no protein or carbonate bands, although at high wavenumbers hydroxyl groups can be identified. Thus, the origin of hydroxylapatite in this sample it is not clear, it could be attributed to traces of the natural mineral as well as to bone ashes as part of the painting recipe.

The specimen of white paint from Galb Budarga has a thick and coarse surface. Its Raman spectra revealed that the dominant component of the paint is anhydrite ($CaSO_4$). This sulphate is the final result of gypsum dehydration after an intermediate phase of bassanite ($CaSO_4 \cdot 0{,}5H_2O$). Nevertheless, there are different types of anhydrite which can be distinguished by Raman spectroscopy: anhydrite III (soluble), anhydrite II (natural or insoluble) and anhydrite I [21]. The stability of these three phases depends on different factors like the dehydration temperature or impurities in the specimen. Anhydrite II is the most abundant phase in the sample of the white pigment, Fig. 3B. However, it is difficult to discriminate the bands from the different polymorphs, Table 2. Bands at 1008 and 1016 cm^{-1} in Fig. 5b may be assigned to the symmetric stretching mode of the sulphate group from two calcium sulphates that coexist in the same specimen. The band at 1008 cm^{-1} is clearly assigned to gypsum. Bands at 1016 and 1128 cm^{-1} can be assigned either to anhydrite I or II, as well as bands at 417, 502, 608, 627 and 675 cm^{-1}. The environmental conditions of the sites in the Western Sahara desert, with an extremely dry climate, could provoke gypsum dehydration. Therefore, rock paintings containing hydrated forms of calcium sulphate exposed to sunlight and wind can exhibit different phases of their dehydration process. Despite this consideration it cannot be declared whether the paints were made only with gypsum or with a mixture containing originally gypsum and anhydrite. Whewellite, ($CaC_2O_4.H_2O$), a hydrated form of calcium oxalate, has been detected in some samples of Galb Budarga site from their Raman spectra, Fig. 3Bb. Crusts of whewellite and weddellite [$CaC_2O_4 (2+x)H_2O$, $x \leq 0.5$] are frequently found on the surface of rock shelters as result of the metabolic activity of lichens, fungi, bacteria and microbes inhabiting their outer layers [22-24]. Layers of these oxalates in close relationship with the paint layers could be used for radiocarbon dating of the pictographs [25,26].

4.2. Tuama Budarga

As indicated previously, five paint specimens of different colours have been extracted from the Tuama Budarga rock shelter. Their colour scheme varies from dark orange to dark red. Small flakes containing paint in one face and rests of substratum in the other have been studied by μ-Raman spectroscopy. The main component of all the Tuama Budarga paint specimens is haematite, Fig. 4. In the case of the specimen TB1, Fig. 4a, the full-width at half height of the Raman bands and the absence of the band at 660 cm^{-1} indicate the presence of very well crystallized haematite. The haematite particles of these specimens have a fine granular size, less than 1 μm. Accretions of whewellite and weddellite are present in all specimens. Hydroxylapatite, Fig. 3Aa, anhydrite, Fig. 3Ba, and the other minerals detected in the rocks of the Galb Budarga shelter have also been observed in this site. The strong and broad D1 and G bands of amorphous carbon at 1344 and 1603 cm^{-1} respectively in the Raman spectra of black micro-particles of the paint, Fig.5b, suggests the addition of this component, charcoal or soot, to the pictorial recipe. Bone black can be excluded due to the absence of the band corresponding to symmetric stretching mode of the phosphate group at ~960 cm^{-1}. Special attention deserves the specimen TB3. Raman spectra of this paint specimen show three bands at 575, 673 and 723 cm^{-1} in the spectral region where bands of manganese oxides (Mn_xO_y) and oxyhydroxides ($Mn_xO_y(OH)_z$) assigned to the Mn–O and Mn–OH bending and stretching vibrations (450-800 cm^{-1}) [27-35] appear, Fig. 6b. The identification of these compounds is frequently difficult [18,36-38] because they have no clear Raman signature due to non-stoichiometric and disordered structures [39]. Their low crystallinity [37], different oxidation states, and the simultaneous presence of different compounds in the same specimen even at microscopic level [38] make the identification even more difficult. Furthermore, manganese oxides/oxyhydroxides may suffer thermal alterations under high laser power values [28,39]. Nevertheless, the observed bands could tentatively be assigned to a mix of birnessite ($Na_{0,3}Ca_{0,1}K_{0,1}(Mn^{4+},Mn^{3+})_2O_4 \cdot 1,5H_2O$) and nsutite ($(Mn^{4+},Mn^{2+})(O,OH)_2$) [28,29,40]. The presence of manganese compounds have been confirmed by SEM/EDX, Fig. 6a. Considerable quantities of haematite and calcium oxalates have also been found in the TB3 specimen. Microstratigraphic analysis of this specimen, Fig. 7, reveals the presence of three different layers over the rocky substratum. The external layer is a thin coating of whewellite with some haematite microparticles, Fig. 7a. The middle layer of red paint contains an important amount of haematite with some particles of whewellite, calcite and amorphous carbon, Fig. 7b. As in the TB1 specimen, very well crystallized haematite has been used as pigment. Only one band at 610 cm^{-1} is observed in the 600-700 cm^{-1} spectral range [41,42], the band at ~660 cm^{-1} is not present, broadening of the band at ~407 cm^{-1} is not observed [36] and the bands at 222, 289 and 608 cm^{-1} are strong and very narrow (their full-width at half height is less than 13 cm^{-1}) [13,32, 40], Fig. 7b. Whewellite and some traces the polyester resin used to prepare the thin cross section for the microstratigraphic study have been detected in the internal layer, Fig. 7c. The paint layer is between two whewellite layers, an opportunity to bracket between *ante quem* and *post quem* radiocarbon dates the pictorial event [25,26].

5. Conclusions

Two different types of paint have been identified in the pictographs of the Galb Budarga and Tuama Budarga rock shelters by μ-Raman spectroscopy. The Galb Budarga shelter is decorated with an unusual white paint containing mainly anhydrite I and II and some gypsum. Crusts of the calcium oxalates whewellite, and weddellite, with some particles of haematite, are also present. The motifs depicted in the Tuama Budarga shelter have been painted in orange-red colours. Haematite is the principal component of the paint used. Small amounts of manganese oxides/oxyhydroxides, tentatively birnessite and nsutite, amorphous carbon and calcite have also been detected in the paint. SEM/EDX analyses confirmed the presence of manganese compounds. The presence of all these components may suggest the use of a pictorial recipe to elaborate the paint. Accretions of whewellite, weddellite, anhydrite, and hydroxylapatite have also been identified in the painting panel of this rock shelter. Three different layers have been identified by microstratigraphic μ-Raman analyses of Tuama Budarga paint specimens. The paint layer, mainly composed by haematite, is between calcium oxalate layers (whewellite, weddellite). Finally, albite, α-quartz, dolomite, gypsum, anhydrite, haematite and hydroxylapatite have been identified in the rocks supporting the paintings of both sites.

6. References

[1] A. Hernanz, Raman spectroscopy of prehistoric pictorial materials, in: P. Bueno, P. Bahn (Eds.), Prehistoric Art as Prehistoric Culture, Archaeopress Archaeology, Oxford, UK, 2015, pp. 11-19.

[2] A. Hernanz, J. Chang, M. Iriarte, J.M. Gavira-Vallejo, R. de Balbín-Behrmann, P. Bueno-Ramírez, A. Maroto-Valiente, Raman microscopy of hand stencils rock art from the Yabrai Mountain, Inner Mongolia Autonomous Region, China, Appl. Phys. A 122:699 (2016) 1-8.

[3] A. Hernanz, M. Iriarte, P. Bueno-Ramírez, R. de Balbín-Behrmann, J.M. Gavira-Vallejo, D. Calderón-Saturio, L. Laporte, R. Barroso-Bermejo, P. Gouezin, A. Maroto-Valiente, L. Salanova, G. Benetau-Douillard, E. Mens, Raman microscopy of prehistoric paintings in French megalithic monuments, J. Raman Spectrosc. 47 (2016) 571-578.

[4] M. Tascon, N. Mastrangelo, L. Gheco, M. Gastaldi, M. Quesada, F. Marte, Micro-spectroscopic analysis of pigments and carbonization layers on prehispanic rock art at the Oyola's caves, Argentina, using a stratigraphic approach, Microchem. J. 129 (2016) 297-304.

[5] A. Hernanz, J.F. Ruiz-López, J.M. Madariaga, E. Gavrilenko, M. Maguregui, S. Fdez-Ortiz de Vallejuelo, I. Martínez-Arkarazo, R. Alloza-Izquierdo, V. Baldellou-Martínez, R. Viñas-Vallverdú, Albert Rubio i Mora, Àfrica Pitarch, A. Giakoumaki, Spectroscopic characterisation of crusts interstratified with prehistoric paintings preserved in open-air rock art shelters, J. Raman Spectrosc. 45 (2014) 1236-1243.

[6] A. Hernanz, J.M. Gavira-Vallejo, J.F. Ruiz-López, H.G.M. Edwards, A comprehensive micro-Raman spectroscopic study of prehistoric rock paintings from the Sierra de las Cuerdas, Cuenca, Spain, J. Raman Spectrosc. 39 (2008) 972-984.
[7] A. Sáenz de Buruaga,. Contribución al conocimiento del pasado cultural del Tiris. Sahara Occidental. Inventario del patrimonio arqueológico, 2005-2007, Servicio Central de Publicaciones del Gobierno Vasco, Departamento de Cultura, Vitoria-Gasteiz, Spain, 2008.
[8] A. Sáenz de Buruaga, Pinceladas de un desierto vivo desde la región del Tiris, en las tierras libres del Sahara Occidental, Servicio Central de Publicaciones del Gobierno Vasco, Departamento de Cultura, Vitoria-Gasteiz, Spain, 2010.
[9] A. Sáenz de Buruaga, Nuevas aportaciones al conocimiento del pasado cultural del Tiris. Sahara Occidental. Inventario del patrimonio arqueológico, 2008-2011, Servicio Central de Publicaciones del Gobierno Vasco, Departamento de Cultura, Vitoria-Gasteiz, Spain, 2014.
[10] J. Soler Subils, The Age and the Natural Context of the Western Sahara Rock Art, International Colloquium *The Signs of Which Times? Chronological and Palaeoenvironmental Issues in the Rock Art of Northern Africa*, Royal Academy of Overseas Sciences, Brussels, 2012, 27-45.
[11] A. Rodrigue, L'art rupestre en Afrique du Nord-Ouest, Krei 13 (2015) 41-74.
[12] A. Sáenz de Buruaga, J.M. Arruabarrena, Un recorrido por las imágenes pintadas y grabadas del Tiris. Arte rupestre y territorio en el extremo suroriental del Sahara Occidental, Asociación Vasco-Saharaui de la Evolución Cultural, Vitoria-Gasteiz, Spain, 2015.
[13] A. Hernanz, M. Mas, B. Gavilán, B. Hernández, Raman microscopy and IR spectroscopy of prehistoric paintings from Los Murciélagos cave (Zuheros, Córdoba, Spain), J. Raman Spectrosc. 37 (2006) 492-497.
[14] A. Hernanz, J.F. Ruiz-López, J.M. Gavira-Vallejo, S. Martin, E. Gavrilenko, Raman microscopy of prehistoric rock paintings from the Hoz de Vicente, Minglanilla, Cuenca, Spain, J. Raman Spectrosc. 41 (2010) 1394-1399.
[15] A.S.T.M. Subcommittee on Raman Spectroscopy. Raman Shift Frequency Standards: McCreery Group Summary (ASTM E 1840). American Society for Testing Materials: Philadelphia, PA; http://www.chem.ualberta.ca/~mccreery/raman.html (last accesed 18.10.17).
[16] F. Ospitali, D.C. Smith, M. Lorblanchet, Preliminary investigations by Raman microscopy of Prehistoric pigments in the wall-painted cave at Roucadour, Quercy, France, J. Raman Spectrosc. 37 (2006) 1063-1071.
[17] A. Hernanz, J.M. Gavira-Vallejo, J.F. Ruiz-López, S. Martin, A. Maroto-Valiente, R. de Balbín-Berhmann, M. Menéndez, J.J. Alcolea González, Spectroscopy of Paleolithic rock paintings from the Tito Bustillo and El Buxu Caves, Asturias, Spain, J. Raman Spectrosc**.** 43 (2012) 1644-1650.
[18] D.C. Smith, M. Bouchard, M. Lorblanchet, An initial Raman Microscopic Investigation of Prehistoric Rock Art in Caves of the Quercy District, S. W. France, J. Raman Spectrosc. 30 (1999) 347-354.

[19] J.D. Pasteris, B. Wopenka, J.J. Freeman, K. Rogers, E. Valsami-Jonesc, J.A.M. van der Houwen, M.J. Silva, Lack of OH in nanocrystalline apatite as a function of degree of atomic order: implications for bones and biomaterials, Biomaterials 25 (2004) 229–238.
[20] B. Wopenka, J.D. Pasteris, A mineralogical perspective on the apatite in bone, Mater. Sci. Eng. C 25 (2005) 131–143.
[21] N. Prieto-Taboada, Gómez-Laserna, I. Martínez-Arkarazo, M.A. Olazábal, J.M. Madariaga, Raman Spectra of the Different Phases in the $CaSO_4$-H_2O System, Anal. Chem. 86 (2014**)** 10131-10137.
[22] W.E. Krumbein, U. Brehm, G. Gerdes, A.A. Gorbushina, G. Levit, K. Palinska, In: Krumbein W.E, Paterson D.W, Zavarzin G.A (eds) *Fossil and Recent Biofilms. A Natural History of Life on Earth. Kluwer Academic Press Publishers, Dordrecht.* 2003.
[23] R.J. Frost, Raman spectroscopy of natural oxalates, Anal. Chem. Acta. 517 (2004) 207-214.
[24] D. Hess, D.J. Coker, J.M. Loutsch, J. Russ, Production of oxalates In Vitro by Microbes Isolated from Rock Surfaces with prehistoric paints in the Lower Pecos Region, Texas, Geoarchaeology. 23 (2008) 3-11.
[25] J.F. Ruiz, M. Mas, A. Hernanz, M.W. Rowe, K.L. Steelman, J.M. Gavira, First radiocarbon dating of oxalate crusts over Spanish prehistoric rock art, Int. Newsl. Rock Art (INORA) 46 (2006) 1-5.
[26] J.F. Ruiz, A. Hernanz, R.A. Armitage, M.W. Rowe, R. Viñas, J.M. Gavira-Vallejo, A. Rubio, Calcium oxalate AMS 14C dating and chronology of Post-Palaeolithic rock paintings in the Iberian Peninsula. Two dates from Abrigo de los Oculados (Henarejos, Cuenca, Spain), J. Archaeol. Sci. 39 (2012) 2655-2667.
[27] F. Buciuman, F. Patras, C. Radu, D.R.T. Zahn, Vibrational spectroscopy of bulk and supported manganese oxides, Phys. Chem. Chem. Phys. 1 (1999) 185-190.
[28] C.M. Julien, M. Massot, R. Baddour-Hadjean, S. Frenger, S. Bach, J.P. Pereira-Ramos, Raman spectra of birnessite manganese dioxides, Solid State Ionics 159 (2003) 345-356.
[29] C.M. Julien, M. Massot, C. Poinsignon, Lattice vibrations of manganese oxides: Part I. Periodic structures, Spectrochim. Acta A 60 (2004) 689-700.
[30] H.-S. Kim, P.C. Stair, Bacterially Produced Manganese Oxide and Todorokite: UV Raman Spectroscopic Comparison, J. Phys. Chem. B 108 (2004) 17019.
[31] H.Y. Xu, S.L. Xu, X.D. Li, H. Wang, H. Yan, Chemical bath deposition of hausmanite Mn_3O_4 thin films, Appl. Surf. Sci. 252 (2006) 4091-4096.
[32] L.-X. Yang, Y.-J. Zhu, H. Tong, W.-W. Wang, G.-F. Cheng, Low temperature synthesis of Mn_3O_4 polyhedral nanocrystals and magnetic study, J. Solid State Chem. 179 (2006) 1225-1229.
[33] N. Mironova-Ulmanea, A. Kuzmina, M. Grubeb, Raman and Infrared spectromicroscopy of manganese oxides, J. Alloys Compd. 480 (2009) 97-99.
[34] S.-H. Shim, D. LaBounty, T.S. Duffy, Raman spectra of bixbyite, Mn_2O_3, up to 40 GPa, Phys. Chem. Minerals 38 (2011) 685.

[35] Z.-Y. Tian, P.M. Kouotou, N. Bahlawane, P.H.T. Ngamou, synthesis of the catalytically active Mn_3O_4 spinel and its thermal properties, J. Phys. Chem. C 117 (2013) 6218-6224.
[36] F. Ospitali, D.C. Smith, M. Lorblanchet, Preliminary investigations by Raman microscopy of prehistoric pigments in the wall-painted cave at Roucadour , Quercy, France, J. Raman Spectrosc. 37 (2006) 1063-1071.
[37] S. Lahlil, M. Lebon, L. Beck, H. Rousselière, C. Vignaud, I. Reiche, M. Menu, P. Paillet, F. Plassard, The first in situ micro-Raman spectroscopic analysis of prehistoric cave art of Rouffignac St-Cernin, France, J. Raman Spectrosc. 43 (2012) 1637.
[38] A. Pitarch, J.F. Ruiz, S. Fdez-Ortiz de Vallejuelo, A. Hernanz, M. Maguregui, J.M. Madariaga, In situ characterization by Raman and X.-ray fluorescence spectrocopy of post-Paleolithic blackish pictographs exposed to the open air in Los Chaparros shelter (Albalate del Arzobispo, Teruel, Spain), Anal. Methods 6 (2014) 6641.
[39] M.C. Bernard, A. Hugot-Le Goff, B. Vu Thi, S. Cordoba de Torresi, Electrochromic reactions in manganese oxides, J. Electrochem. Soc. 140 (1993) 3065.
[40] E. Cerrillo Cuenca, M. Sepúlveda., An assessment of methods for the digital enhancement of rock paintings: the rock art from the precordillera of Africa (Chile) as a case study, J. Archaeol. Sci. 55 (2015) 197.
[41] D.L.A. de Faria, S.V. Silva, M.T. de Oliveira, Raman microspectrocopy of some iron oxides and oxyhydroxides, J. Raman Spectrosc 28 (1997) 873-878.
[42] L. Wang, J. Zhu, Y. Yan, Y. Xie, C. Wang, Micro-structural characterization of red decorations of red and green color porcelain (honglvcai) in China, J. Raman Spectros. 40 (2009) 998-1003.

403

Table 1. Identified compounds in rock substrata, accretions and paintings in African sites by μ-Raman

Site	Specimen	Rock substrata and accretions	Paintings
Galb Budarga	GB1 substratum	α-Quartz, albite, dolomite, haematite, anhydrite, gypsum, hidroxylapatite	--
	GB2 white pigment	Whewellite, gypsum	Anhydrite
Tuama Budarga	TB1 pale orange pigment	α-Quartz, albite, weddellite, gypsum, anhydrite	Haematite
	TB2 dark red pigment	Whewellite, weddellite	Haematite, amorphous carbon
	TB3 red pigment	Whewellite, gypsum, manganese oxide/oxihydroxide	Haematite, amorphous carbon
	TB4 red pigment	Albite, gypsum, anhydrite	Haematite
	TB5 orange pigment	Albite, hidroxylapatite, gypsum, anhydrite	Haematite

404

Table 2. Raman bands of calcium sulphates polymorphs [21] and those from the Galb Budarga white paint (GB2)

Active Raman modes	Gypsum /cm^{-1}	Bassanite / cm^{-1}	Anhydrite III /cm^{-1}	Anhydrite II /cm^{-1}	Anhydrite I /cm^{-1}	GB2
ν_2	415, 495	428, 489	420, 490	**417, 499**	**417**, 497	418, 500
ν_4	620, 673	627, 669	630, 673	**609, 628, 675**	**609, 628, 676**	610, 628, 676
ν_1	1008	1015	1025	**1017**	**1017**	1017
ν_3	1134	1128	1167	**1111, 1128,** 1160	1108, 1127, **1158**	1112, 1128, 1158

405 Wavenumbers in bold correspond to Raman bands of calcium sulphates close to those of the Galb
406 Budarga white pigment.

407

Figure legends

Figure 1. a, zoomorphic motifs from the Galb Budarga rock shelter. The scale is 30 cm in length; b, c, d, e, pictographs from the Tuama Budarga rock shelter. The scales are 10 cm in length.

Figure 2. Galb Budarga Raman spectra from the specimen GB1. Labels: alb, albite; h, haematite and gy, gypsum.

Figure 3. A, Raman spectra of white paint from the Galb Budarga shelter. Labels: anh, anhydrite II; w, whewellite; gy, gypsum; B, selected and representative Raman spectra from the rocky substrata and accretions of the painting panels of both sites: a, Tuama Budarga shelter; b, Galb Budarga shelter. Labels: hAp, hydroxylapatite; wd, weddellite; w, whewellite.

Figure 4. Representative Raman spectra from Tuama Budarga paint specimens: a, TB1; b, TB4; c, TB5; d, TB3 and e, TB2. Labels: h, haematite; w, whewellite.

Figure 5. Representative Raman spectra from the Tuama Budarga: a, TB1; b, TB2 and c, TB1. Labels: alb, albite; wd, weddellite; w, whewellite; ac, amorphous carbon; anh, anhydrite; h, haematite.

Figure 6. a, EDX spectra and SEM image of the TB3 specimen from Tuama Budarga shelter. Ni and Cu peaks are from the metallic sample holder; b, representative Raman spectrum of the paint specimen TB3 from the Tuama Budarga rock shelter. Labels: bir, birnessite; nsu, nsutite.

Figure 7. (Up) Microphotograph with polarized light of a polished thin section (30 μm) of a small flake from the specimen TB3; a, external layer; b, paint layer; c, internal layer. (Down) Raman spectra from each (a, b, c) microstratigraphic layers. Labels: h, haematite; w, whewellite; ca, calcite; ac, amorphous carbon; res, polyester resin.

Figure 1. a, zoomorphic motifs from the Galb Budarga rock shelter. The scale is 30 cm in length; b, c, d, e, pictographs from the Tuama Budarga rock shelter. The scales are 10 cm in length.

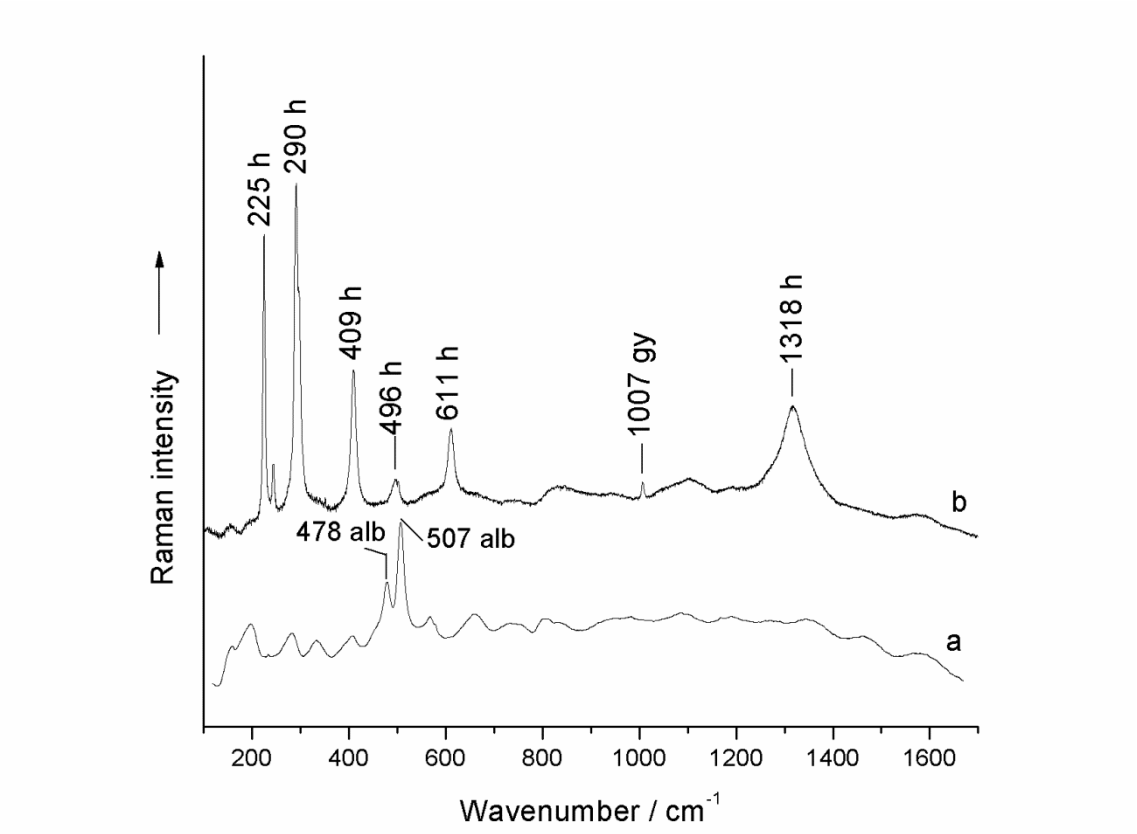

Figure 2. Galb Budarga Raman spectra from the specimen GB1. Labels: alb, albite; h, haematite and gy, gypsum.

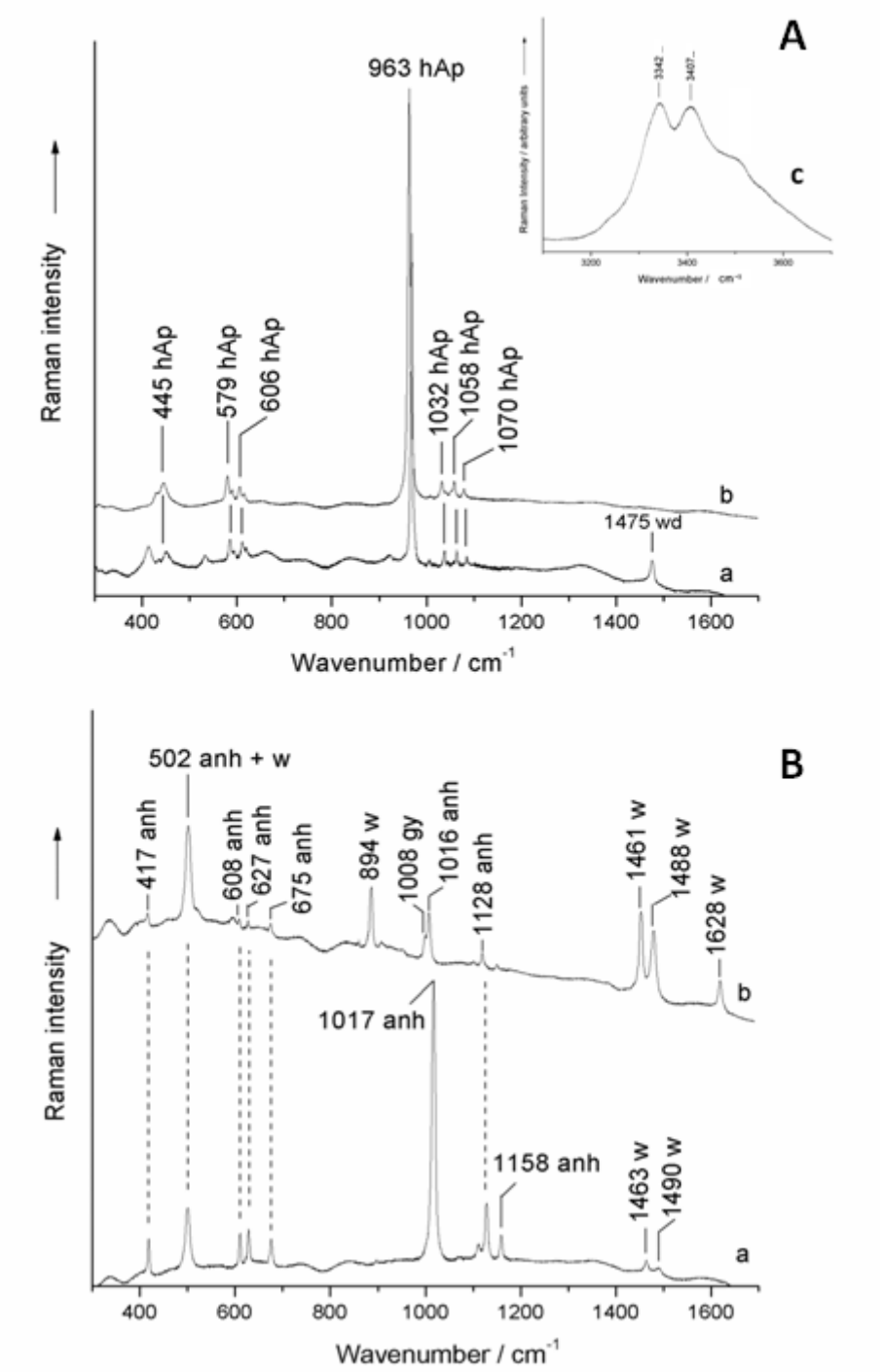

Figure 3. A, Raman spectra of white paint from the Galb Budarga shelter. Labels: anh, anhydrite II; w, whewellite; gy, gypsum; B, selected and representative Raman spectra from the rocky substrata and accretions of the painting panels of both sites: a, Tuama Budarga shelter; b, Galb Budarga shelter. Labels: hAp, hydroxylapatite; wd, weddellite; w, whewellite.

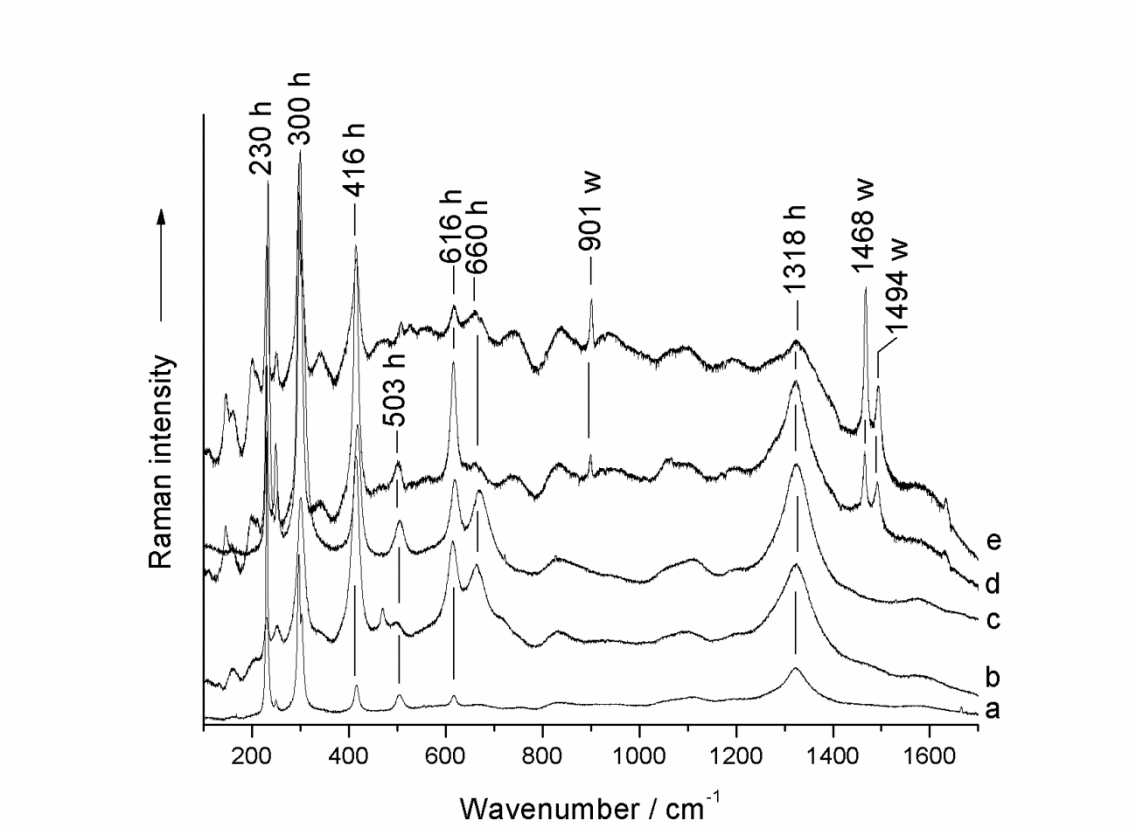

452

453 **Figure 4**. Representative Raman spectra from Tuama Budarga paint specimens: a, TB1;
454 b, TB4; c, TB5; d, TB3 and e, TB2. Labels: h, haematite; w, whewellite.

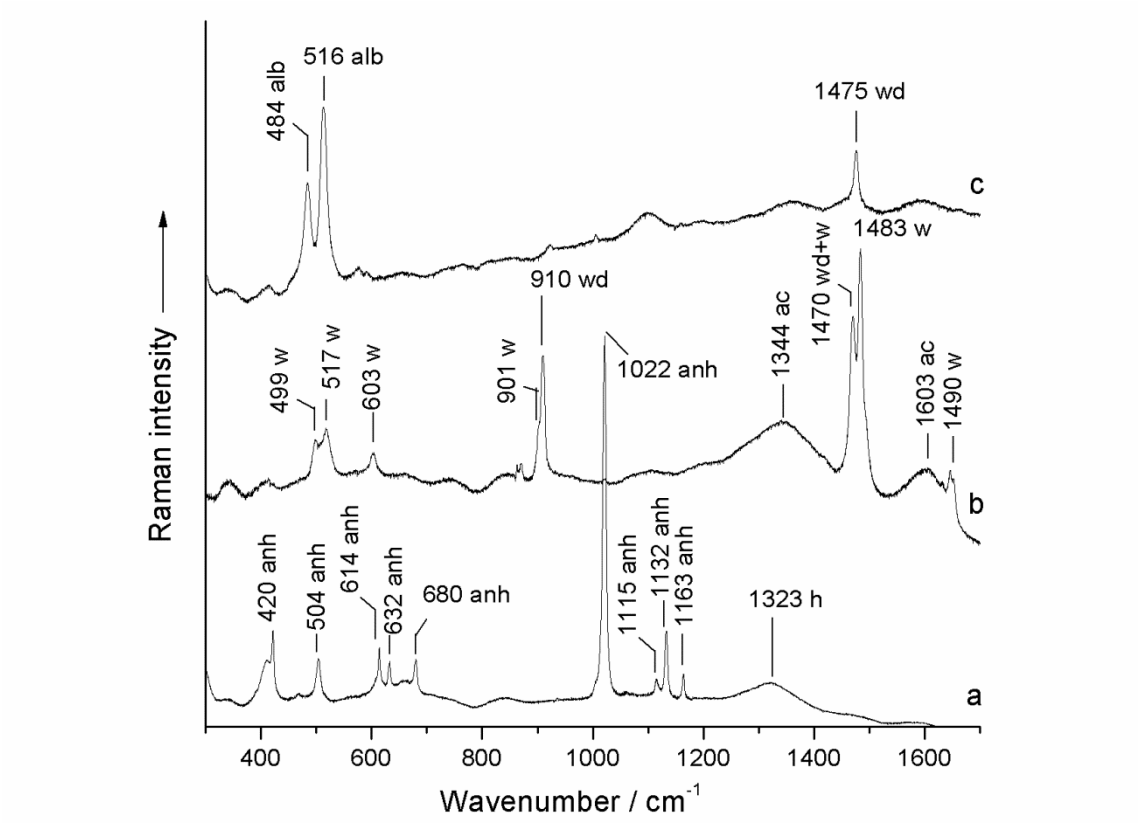

455

456 **Figure 5**. Representative Raman spectra from the Tuama Budarga: a, TB1; b, TB2 and
457 c, TB1. Labels: alb, albite; wd, weddellite; w, whewellite; ac, amorphous
458 carbon; anh, anhydrite; h, haematite.

459

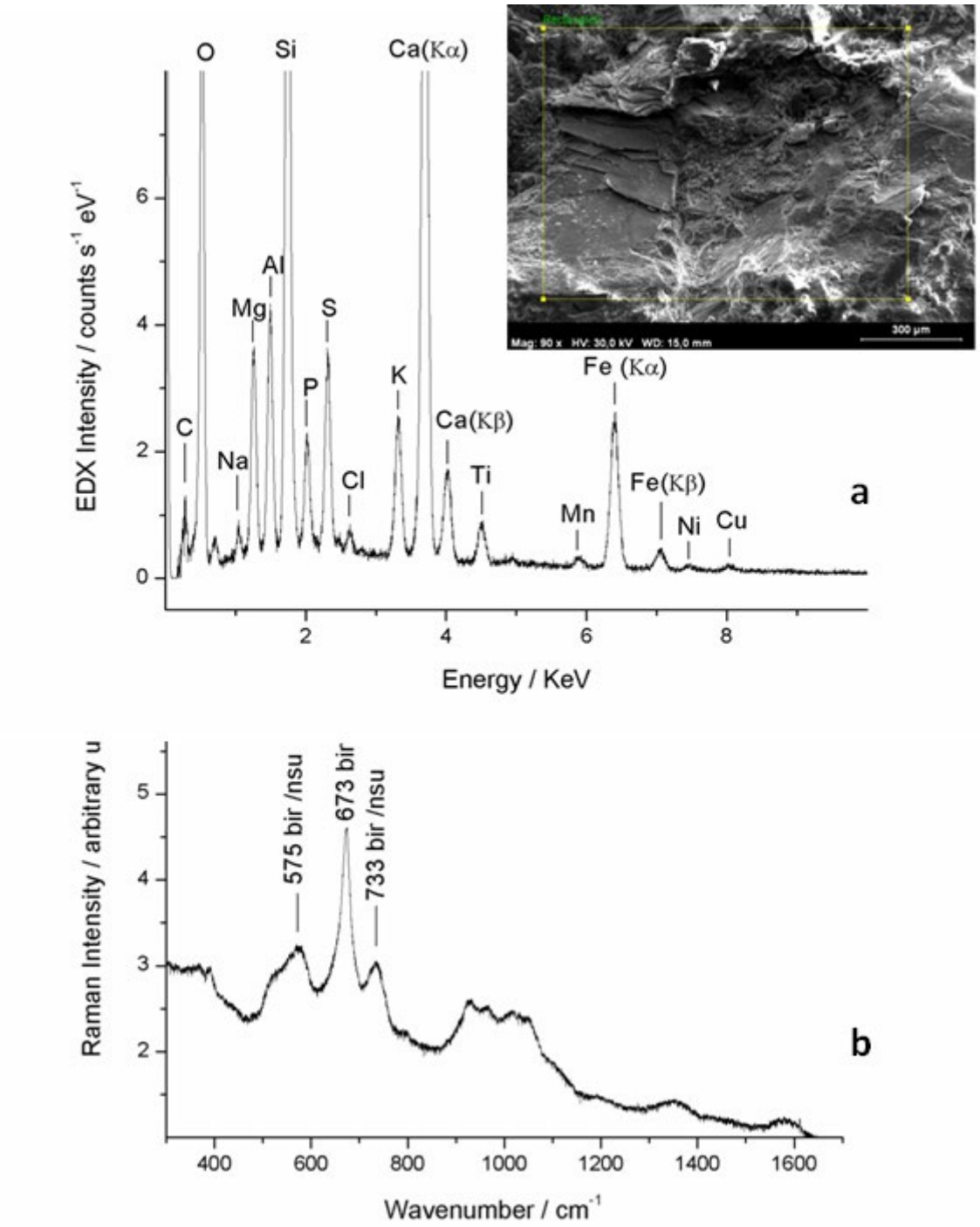

460

461 **Figure 6**. a, EDX spectra and SEM image of the TB3 specimen from Tuama Budarga
462 shelter. Ni and Cu peaks are from the metallic sample holder; b,
463 representative Raman spectrum of the paint specimen TB3 from the Tuama
464 Budarga rock shelter. Labels: bir, birnessite; nsu, nsutite.

465

466

467

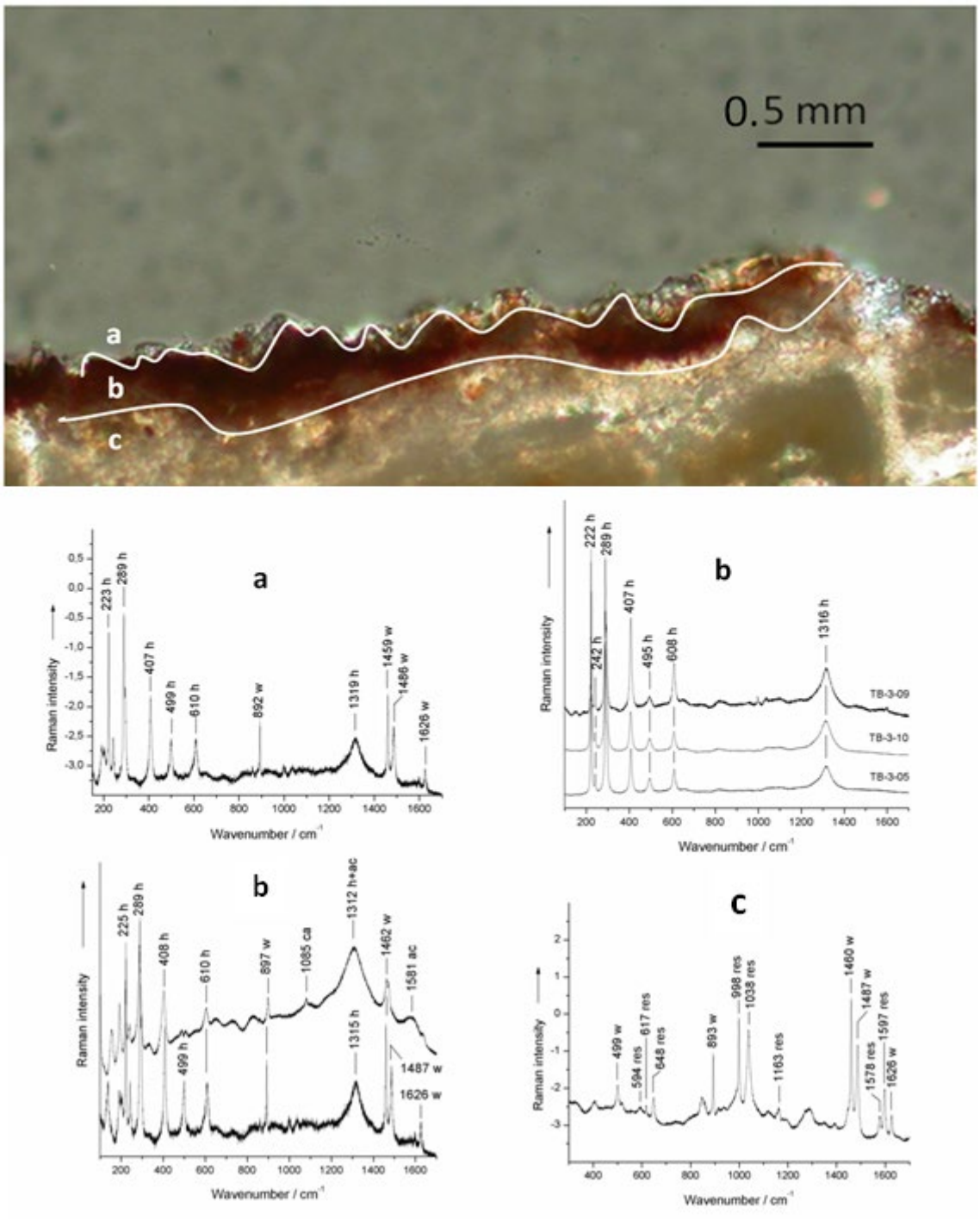

Figure 7. Up, microphotograph with polarized light of a polished thin section (30 μm) of a small flake from the specimen TB3; a, external layer; b, paint layer; c, internal layer. Below, Raman spectra from each (a, b, c) microstratigraphic layers. Labels: h, haematite; w, whewellite; ca, calcite; ac, amorphous carbon; res, polyester resin.